

# Adversarial Detection by Approximation of Ensemble Boundary

Terry Windeatt

Centre for Vision, Speech and Signal Processing (CVSSP), University of  
Surrey, Guildford, Surrey, UK, GU2 7XH .

Contributing authors: [t.windeatt@surrey.ac.uk](mailto:t.windeatt@surrey.ac.uk);

## Abstract

A new method of detecting adversarial attacks is proposed for an ensemble of *Deep Neural Networks (DNNs)* solving two-class pattern recognition problems. The ensemble is combined using Walsh coefficients which are capable of approximating Boolean functions and thereby controlling the complexity of the ensemble decision boundary. The hypothesis in this paper is that decision boundaries with high curvature allow adversarial perturbations to be found, but change the curvature of the decision boundary, which is then approximated in a different way by Walsh coefficients compared to the clean images. By observing the difference in Walsh coefficient approximation between clean and adversarial images, it is shown experimentally that transferability of attack may be used for detection. Furthermore, approximating the decision boundary may aid in understanding the learning and transferability properties of *DNNs*. While the experiments here use images, the proposed approach of modelling two-class ensemble decision boundaries could in principle be applied to any application area. Code for approximating Boolean functions using Walsh coefficients: <https://doi.org/10.24433/CO.3695905.v1>

**Keywords:** Adversarial robustness, Boolean functions, Ensemble, Deep neural networks, Machine learning, Security

## 1 Introduction

Despite achieving excellent performance in many application areas, *Deep Neural Networks (DNNs)* are known to be susceptible to being fooled [1] [2]. This can take many

forms in various applications but visually is most striking when an image is manipulated, so that the *DNN* misclassifies although the required perturbation results in an image that appears no different to a human. The perturbation is computed in various ways and known as adversarial pattern generation or adversarial attack. Example images of this phenomenon can be found, for example in He et al. [3]. Although the attack usually consists of a digital manipulation, it can also be physical [4]. Lack of susceptibility to adversarial attacks is known as adversarial robustness and is clearly a desirable property.

Besides having important practical implications, especially for security and safety-related applications [3] the problem of adversarial attacks has been extensively studied theoretically. However, the existence of adversarial examples appears still to be a mystery [2]. Indeed, there is recent recognition that adversarial pattern generation can help explain how *DNNs* learn, which would be important since there are many aspects of *DNN* learning which are poorly understood and remain open research questions [5]. The main idea is that an adversarial attack, which attempts to push a pattern on the other side of a decision boundary, gives a notion of how the boundary is behaving during learning.

As a result of the practical issue of the threat to *DNNs*, adversarial attacks and subsequent defences have become somewhat of a game. At present it appears that the attackers are winning, since there is evidence that the current adversarial defences that claim to be robust, can all be defeated [6] [3]. The most successful defence is adversarial training, in which the original training set is enhanced with adversarial patterns. However, reducing the computational cost of adversarial training to make it a practical solution is an open research question [2].

Ensembles or multiple classifier systems are a well-recognised method of solving pattern recognition problems. The two main phases in ensemble design are classifier generation and combination. Classifier generation (known as individual or base classifiers) has the aim of producing accurate yet diverse classifiers, although diversity has remained an elusive concept from the early days of ensembles up to the present [7] [8]. The combination phase is usually simple, such as a *Majority Vote* or *Weighted Vote*. Weighted combination rules have been extensively investigated but there is no established strategy for computing the weights. Trainable rules have been developed, but it is not clear whether there is any advantage and the training parameters can be difficult to set. When applied to *DNNs*, there is a belief that ensembles have limited usefulness, because single state-of-the-art *DNNs* achieve remarkable performance by themselves without the need for combining diverse individuals [9]. However, some researchers still claim that ensembles can improve adversarial detection [1].

In this paper, an ensemble of parallel *DNNs* is proposed for approximating the decision boundary using Walsh spectral coefficients, and thereby detecting adversarial attacks. Walsh coefficients were first proposed for pattern recognition in the 1970's [10], although the assumption was that the classifier inputs were binary features rather than class labels as inputs to a combining rule. Like *Majority Vote*, only class labels are used for Walsh spectral coefficients. The only parameter to choose in the Walsh combination is the order of the coefficients, which acts as a form of regularisation [11] and determines how well the ensemble boundary is approximated. Section 2 describes

**Table 1** Rademacher-Walsh Polynomial Functions  
(order  $N \leq 4$ )

$j$	$\phi_j(X)$
1	1
2	$2x_1 - 1$
3	$2x_2 - 1$
$\vdots$	$\vdots$
$N + 1$	$2x_N - 1$
$N + 2$	$(2x_1 - 1)(2x_2 - 1)$
$N + 3$	$(2x_1 - 1)(2x_3 - 1)$
$\vdots$	$\vdots$
$N + 2 + N - 1$	$(2x_1 - 1)(2x_N - 1)$
$N + 3 + N - 1$	$(2x_2 - 1)(2x_3 - 1)$
$\vdots$	$\vdots$
$N + 2 + N(N - 1)/2$	$(2x_{N-1} - 1)(2x_N - 1)$
$N + 3 + N(N - 1)/2$	$(2x_1 - 1)(2x_2 - 1)(2x_3 - 1)$
$\vdots$	$\vdots$
$2^N$	$(2x_1 - 1)(2x_2 - 1) \dots (2x_N - 1)$

how Walsh coefficients may be used for the combining rule of a classifier ensemble and shows that *Weighted Vote* is a special case of Walsh approximation.

## 2 Ensembles Combined using Walsh Coefficients

In this paper, *DNNs* are used as base classifiers in an ensemble that solves two-class classification problems. It is assumed that there are  $N$  parallel base classifiers, with final layer of each *DNN* providing a binary classification. Let  $X_m$  be the  $N$ -dimensional binary vector that represents the decisions of the  $N$  *DNN* classifiers for the  $m^{th}$  pattern. If the target label for the  $m^{th}$  pattern is denoted by  $\Omega_m$  then  $\Omega_m = \varphi(X_m)$  where  $m = 1 \dots \mu$ ,  $\Omega_m \in \{0,1\}$  and  $\varphi$  is the unknown Boolean function that maps  $X_m$  to  $\Omega_m$ . Each element of  $X_m$  represents a vertex in the  $N$ -dimensional binary hypercube.

Following Tou & Gonzales [10], the discrete probability density function can be approximated using *Rademacher-Walsh (RW)* polynomials as orthogonal basis functions. Therefore, in the context of an ensemble the probability of occurrence of each of the  $\mu$  binary votes is computed. The *RW* polynomials contain  $2^N$  possible terms and are formed by taking products as shown in Table 1 for  $N \leq 4$  (The full table of the *RW* polynomials for  $N > 4$ , and an explanation of how they may be used, can be found in chapter 4.6.4 in Tou & Gonzales [10]). *RW* discrete polynomial functions are orthogonal, satisfying the property that

$$\sum_{m=1}^{2^N} \phi_j(X_m) = \begin{cases} 2^N & \text{if } j = k \\ 0 & \text{if } j \neq k \end{cases} \quad (1)$$

An approximation of the discrete probability density  $p$  using  $q$  basis functions and  $\mu$  patterns is given by

$$\hat{p} = \sum_{j=1}^q \chi_j \phi_j(X) \quad (2)$$

where coefficients are given by

$$\chi_k = \frac{1}{2^N \mu} \sum_{i=1}^{\mu} \phi_k(X_i) \quad (3)$$

Spectral coefficients may also be interpreted as correlation with class labels [12]. The first order coefficients,  $j = 2 \dots N+1$  in Table 1 represent the correlation with the class label. Second and higher order coefficients represent correlation with the logic *exclusive-OR* ( $xor$  denoted  $\oplus$ ) of the respective coefficients. For example, if  $j = N+2$  in Table 1, the second order spectral coefficient  $s_{12}$  is given by

$$s_{12} = \chi_5 = \frac{1}{2^N \mu} \sum_{m=1}^{\mu} C(x_{m1} \oplus x_{m2}, \Omega_m) \quad (4)$$

$$\text{where } C(a, b) = \begin{cases} +1 & \text{if } a = b \\ -1 & \text{if } a \neq b \end{cases}$$

A simple example shows how to compute the three combinations of the second order contribution for a three-dimensional binary pattern  $[x_1, x_2, x_3] = [0, 1, 1]$ . With reference to Table 1 and (2) and (3), for  $[x_1, x_2]$  the basis function is  $(2x_1-1)(2x_2-1) = (-1)(1) = -1$ . Similarly, for  $[x_1, x_3]$  the count is -1 but for  $[x_2, x_3]$  the count is +1. Adding the three contributions gives a count of -1 for that pattern. There are eight basis functions in total (from (1) with  $N = 3$ ), the remaining being  $0^{th}$ ,  $1^{st}$  and  $3^{rd}$  order.

To compute the probability estimate of two classes  $\omega_1, \omega_0$  assume prior probability is given by the number of patterns. A decision function  $d(X)$  is formed by subtracting the probability estimate of the two classes, which is the probability density in (2) multiplied by prior probability:

$$d(X) = \hat{p}(X | \omega_1)p(\omega_1) - \hat{p}(X | \omega_0)p(\omega_0) \quad (5)$$

After normalising (5), the Walsh decision probability is used in Section 4.2. Note that the two probability estimates in (5) contain the same divisor ( $2^N$ ) in (3), so can be ignored when computing the decision function. The decision function based on the Walsh coefficient combiner of order  $y$  is defined as  $W_y$ , so third order is  $W_3$ , and contains the addition of contributions from  $W_0, W_1, W_2$ . Note from Table 1 that  $W_0$  basis function ( $j=1$ ) is constant and does not depend on the pattern elements. So  $W_0$  is just the difference of the number of patterns in the two classes.  $W_1$  is similar to an

ensemble weighted vote with weights set by correlation of individual classifiers with class label.

### 3 Adversarial robustness

Adversarial examples were first demonstrated in Szegedy et al. [13] and Biggio et al. [14]. In this paper, the focus is limited to adversarial robustness, as applied to images. The intention of an adversarial attack is to perturb an image so that it is misclassified, yet to the human eye appears little or no different. It is an interesting topic theoretically, because it shows the limitations of machine learning applied to images. From a practical standpoint, for an application that is safety or security related a misclassification could incur a high cost e.g. a self-driving car, that misclassifies a pedestrian. It is not obvious why human invisible adversarial perturbations provide a successful attack. However, perhaps it is not surprising because *DNNs* generally learn using backpropagation, which is not biologically plausible. Indeed, some have questioned whether a different learning algorithm would need to be developed, more in line with the way humans learn [15] [2].

In the context of images, there are many theories as to why *DNNs* are not robust to adversarial pattern generation. Goodfellow et al. [16] argue that gradient-based optimisation requires *DNN* classifiers to be designed to be sufficiently linear, and that this local linearity causes susceptibility to adversarial examples and the transference to different classifiers. The theoretical analysis in Shafahi et al. [17] identifies fundamental bounds on the susceptibility of a classifier to adversarial attacks, and concludes that adversarial examples may be inevitable. The analysis in Schmidt et al. [18] links adversarially robust generalisation to over-fitting, arguing that depending on the particular dataset distribution, more data may be needed. In Fawzi et al. [19], by improving the robustness to random noise, a relationship between robustness and curvature of the decision boundary is established, suggesting that geometric constraints on the curvature of the decision boundary should be imposed.

Many theories, either explicitly or implicitly through the data distribution, link adversarial robustness to the decision boundary [3] [20]. A visual illustration of adversarial patterns close to the decision boundary can be found in Crecchi et al. [21]. Other theories relate robustness to features rather than geometric perspective [22]. For example, in Ilyas et al. [23], features in the final layer of the *DNN* are shown to be split into robust and non-robust features, the former being aligned with the visual features used by humans. Although there are many theories of why *DNNs* are not adversarially robust, the focus here is on the boundary theory.

Adversarial defences have in some cases been based upon ensembles [24] [25] [26]. However, the consensus appears to be that ensembles do not provide defences that cannot be broken by adaptive attacks [27] [6] [9]. An ensemble combined by Walsh coefficients is different in that a complex boundary can be approximated by much simpler classifiers. This is demonstrated in Windeatt et al. [28] for the artificial 2D circular dataset problem, in which simple individual classifiers under-fit, yet  $W_3$  provides a good approximation to the optimal Bayes boundary, while *Majority Vote* and  $W_1$  do not.

The hypothesis in this paper is that decision boundaries with high curvature allow adversarial perturbations to be found, but change the curvature of the decision boundary, which is then approximated in a different way by Walsh coefficients compared to the clean images. A well-established and useful model for understanding ensemble behaviour for two-class problems was formulated in Tumer & Ghosh [29], in which the assumption is made that the distribution of both classes is Gaussian. The relationship between the ensemble model and Walsh coefficients was subsequently used for ensemble design [30] [31]. The conventional wisdom is that if a classifier is too complex, achieving a very low or zero training error rate, then the patterns under the tails of the distribution are correctly classified, leading to a decision boundary that differs from the optimal Bayes boundary, and generalises poorly through over-fitting. Apparently, a *DNN* can produce a decision boundary capable of correctly classifying patterns under the tail, yet still perform well on the test set. A possible reason is that high curvature of decision boundaries enables the patterns to be correctly classified, with boundaries such that other test error patterns in the vicinity are not misclassified. Imagine that each pattern in the overlap area is correctly classified via its own highly curved, possibly disconnected boundary. If the boundary is very tight, it would not affect generalisation, yet could be easily perturbed to misclassify. The visualisations of highly curved decision boundaries in Ortiz-Jiménez et al. [5] and Fawzi et al. [19] suggest that this may be the case. The difficulty is that the space is high-dimensional and there is no guarantee that 2D visualisations are giving a true picture. It is better perhaps to think of it as a tool to try to help understand in an intuitive sense the reason for the relationship between accuracy and robustness.

Experiments described in Section 4 are based on checking adversarial detection for several adversarial attacks (*ADVs*) that use a variety of attack methods. The *ADVs* considered were *Carlini-Wagner*, *ElasticNet*, *HopSkipJump*, *Zeroth Order Optimisation*, along with the five chosen below and all described in Nicolae et al. [32]. In Section 4, *dog/cat(d/c)* is chosen as the most difficult *CIFAR10* [33] problem in terms of error rate. The following *ADVs* used for experiments in Section 4 and implemented in Nicolae et al. [32], were chosen based on their attack success on the *d/c* dataset with default parameters selected: *Deepfool (DF)* [34], *Projection Gradient Descent (PG)* [35], *Universal Adversarial Perturbation (UA)* [36], *Fast Gradient Sign Method (FG)* [37], *Basic Iterative Method (BI)* [37]. While it was possible to increase attack success of the *ADVs* by increasing perturbation levels, the attacks generally produced noticeable visual distortion of the images.

*ADVs* may be classified according to attacker goal, knowledge and strategy [27]. The goal is targeted versus untargeted, the former referring to an attack aimed at misclassifying a specified class, while the latter allows any misclassification. Normally multi-class problems are assumed, but since only two class problems are considered in this paper, the attack is targeted, which is a more difficult problem [38]. Attacker knowledge is either white box or black box. White box assumes that the attacker has complete knowledge of the classifier and parameters, while black box relies on the transferability of attack images produced by a classifier that is in general different from the target classifier. All attacks considered in Section 4 are white box. Attacker strategy is split into additive noise and geometric distortions (such as rotation and

translation to induce misclassifications). All attacks considered here rely on additive noise, either using optimisation algorithms (*PG*, *DF*, *UA*) or simpler and faster sensitivity analysis to determine the contribution of each input feature, for example *gradient descent* or *Jacobian matrix*.

Adversarial defences are based on input transformation, adversarial detection or architectural design [27]. A defence based on Walsh approximation would be considered an adversarial detection approach. It requires a rejection threshold to be set, similar to many defences, for example, Kwon et al. [39], which is based on finding a classification score threshold.

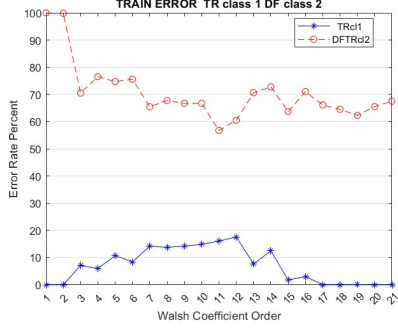
## 4 Experimental evidence

### 4.1 Data-sets and classifiers

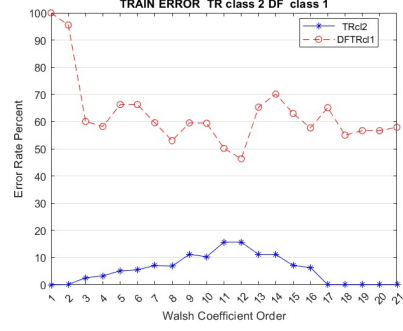
The experiments are designed to test the hypothesis that a Walsh coefficient approximation of an ensemble boundary allows a relatively weak *DNN* classifier combination to detect adversarial images. In order to establish detection ability, the difference in approximation between clean and adversarial images is measured as Walsh coefficient order is increased. The results for the ensemble give recognition rates higher than the average of individual classifiers and close to optimal performance. The classifier architecture for  $32 \times 32 \times 3$  images consists of the following twenty layers:

*32 3×3 convolutions with stride [1 1] and padding 'same'*  
*ReLU*  
*32 3×3 convolutions with stride [1 1] and padding [0 0 0 0]*  
*ReLU*  
*2×2 max pooling with stride [2 2] and padding [0 0 0 0]*  
*25% dropout*  
*64 3×3 convolutions with stride [1 1] and padding same'*  
*ReLU*  
*64 3×3 convolutions with stride [1 1] and padding [0 0 0 0]*  
*ReLU*  
*2×2 max pooling with stride [2 2] and padding [0 0 0 0]*  
*25% dropout*  
*Flatten activations into 1-D*  
*512 fully connected layer*  
*ReLU*  
*50% dropout*  
*2 fully connected layer*  
*Softmax*  
*Classification Output.*

Various two-class problems were chosen according to difficulty from *CIFAR10*, *dog/-cat* (*d/c*), *truck/auto*(*t/a*), *horse/deer*(*h/d*), *frog/cat*(*f/c*), *deer/bird*(*d/b*) and from *MNIST* digit recognition [40]  $9/4$ ,  $7/2$ ,  $9/7$ ,  $8/5$ ,  $8/3$ .

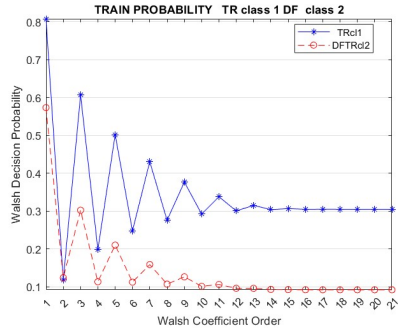


(a) Class 1: *dog* and Class 2: *cat*

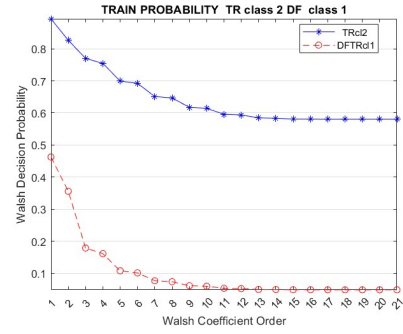


(b) Class 1: *cat* and Class 2: *dog*

**Fig. 1** Train error versus Walsh coefficient order



(a) Class 1: *dog* and Class 2: *cat*



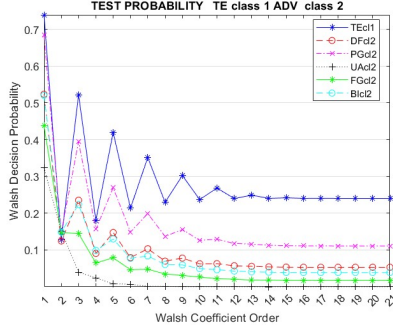
(b) Class 1: *cat* and Class 2: *dog*

**Fig. 2** Walsh decision probability versus coefficient order for Train *Deepfool*(DF)

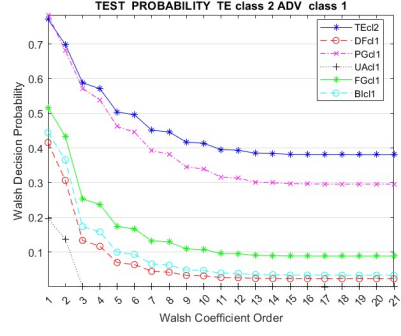
Training uses gradient descent with *adam* optimiser. The ensemble has twenty-one base classifiers, since it was found experimentally that increasing the number beyond twenty-one did not improve or decrease performance for the datasets and number of training patterns considered here. The diversity in each base classifier of the ensemble is due to random starting weights and drop-out.

Classifier parameters were selected based on *d/c*, which is the most difficult two-class problem in *CIFAR10*, and then fixed for testing other two-class problems. The main parameters to set are the number of training epochs, number of nodes in the final layer and the drop-out rate. These were selected as 30, 512 and 50 percent respectively. It was found that varying the number of epochs/nodes and drop-out rate did not significantly alter performance.





(a) Class 1: *dog* and Class 2: *cat*



(b) Class 1: *cat* and Class 2: *dog*

**Fig. 3** Walsh decision probability versus coefficient order for Test and five *ADV*s

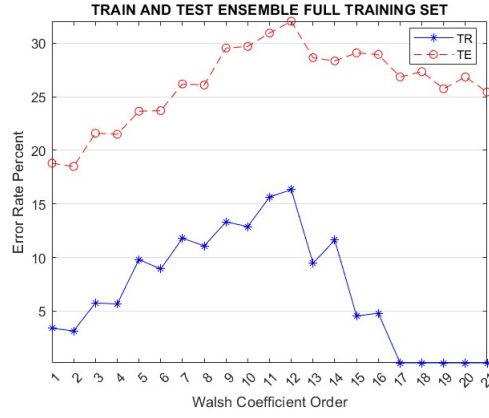


**Fig. 4** Ensemble train and test error of *dog/cat* versus Walsh coefficient order

**Table 2** CIFAR10 optimal *TEACC/ADVREJ* each entry:  
*TECL1/ADVCL2* | *TECL2/ADVCL1*

<i>Pro</i>	<i>DF</i>	<i>PG</i>	<i>UA</i>	<i>FG</i>	<i>BI</i>
d/c	87 93	85 94	90 87	85 86	85 85
t/a	93 93	89 94	— 95	91 94	85 94
h/d	94 92	96 91	96 —	96 79	95 78
f/c	— 94	— 92	— 95	95 93	93 93
d/b	91 94	91 95	92 —	93 92	92 94
Ave	91 93	90 93	93 92	92 89	90 89

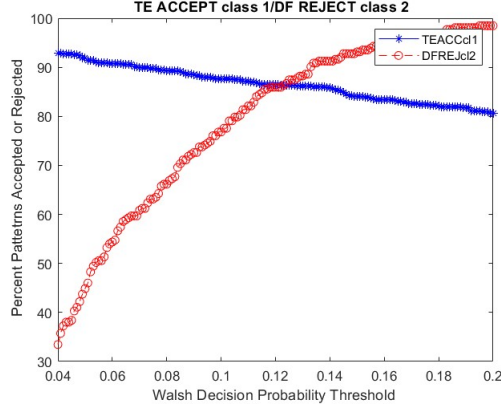


**Fig. 5** Typical TEACC/ADVREJ curve as  $W_1/W_2$  detection threshold is varied

**Table 3** CIFAR10 optimal *TEACC/ADVREJ* using probability threshold from *ADV* (shown bold)

top 5 rows: *TECL1/ADVCL2*

bottom 5 rows: *TECL2/ADVCL1*

<i>Pro</i>	<i>DF</i>	<i>PG</i>	<i>UA</i>	<i>FG</i>	<i>BI</i>
d/c	<b>87</b>	85/85	86/99	85/85	86/84
t/a	<b>93</b>	93/71	-	93/78	91/55
h/d	<b>94</b>	94/98	94/98	94/98	94/96
f/c	-	-	-	<b>95</b>	95/90
d/b	<b>91</b>	91/91	90/100	91/98	91/97
d/c	<b>93</b>	93/95	86/98	87/85	86/84
t/a	<b>93</b>	93/99	94/97	93/96	93/95
h/d	<b>92</b>	91/91	-	78/88	75/90
f/c	<b>94</b>	94/90	94/99	94/92	94/92
d/b	<b>94</b>	94/99	-	94/91	94/94

**Table 4** CIFAR10 optimal *TECL1/ADVCL2* using *majority vote*

<i>Pro</i>	<i>DF</i>	<i>PG</i>	<i>UA</i>	<i>FG</i>	<i>BI</i>
d/c	74	55	85	65	70
t/a	90	85	-	85	80
h/d	82	60	55	75	72
f/c	-	-	-	85	80
d/b	80	70	77	84	80
Ave	81	67	72	79	76

**Table 5** MNIST probability/RANGE x 100 for  
 $i$  *TEACC/ADVREJ* OF 98/98 PERCENT  
top 5 rows: *TECL1/ADVCL2*  
bottom 5 rows: *TECL2/ADVCL1*

<i>Pro</i>	<i>DF</i>	<i>PG</i>	<i>UA</i>	<i>FG</i>	<i>BI</i>
9/4	2/12	2/12	3/12	2/13	2/13
7/2	5/24	5/25	5/24	5/24	5/25
9/7	62/38	62/38	62/38	62/38	62/38
8/5	8/37	8/37	-	6/38	8/37
8/3	7/28	7/28	7/34	7/28	7/28
9/4	9/15	9/15	8/22	9/15	9/15
7/2	6/39	7/35	4/61	6/39	6/44
9/7	6/32	6/32	-	5/32	5/34
8/5	48/52	48/52	48/52	48/52	48/52
8/3	4/20	3/21	4/20	4/20	4/21

## 4.2 Experimental results for *DNN* ensemble

The purpose of the experiments is to find a measure based on Walsh coefficients that is able to distinguish between clean and adversarial images. As explained below, two measures are chosen  $W_2$  and the difference between  $W_1$  and  $W_2$  ( $W_1/W_2$ ). The aim is to find a threshold for the Walsh decision probability (normalised from (5)) that optimises the accuracy of clean image acceptance and adversarial rejection. The Figures in this section relate to *dog/cat* problem, while Tables give results for all the *CIFAR10* and *MNIST* problems defined in Section 4.1.

The nomenclature for this section is as follows: *ADvs DF,PG,UA,FG,BI* are defined in Section 3 and use default parameters as given in Nicolae et al. [32], except that for *FG,BI* a value of twenty is used for epsilon. The Walsh coefficient order  $W_y$  is defined in Section 2. *TE* and *TR* refer to the clean test and training images, respectively, while *ADVTE* and *ADVTR* refer to the adversarial perturbed images e.g. *DFTR* refers to *DeepFool(DF)* training images. Class 1 and 2 are abbreviated as *cl1* and *cl2*, so for example *TEcl1* refers to class 1 of the clean test images. Note that *TEcl1* is compared with *ADVcl2* since both *TE* and *ADV* images are predicted class 1. Similarly *TEcl2* is compared with *ADVcl1*. For experiments in this paper, the goal of adversarial detection is to maximise both the percentage of *TE* images accepted, denoted *TEACC* and the percentage of *ADV* images rejected, denoted *ADVREJ*.

In order to achieve the most reliable results for *TEACC* and *ADVREJ*, both *TR* and *TE* are split such that the clean image is retained if correctly classified by *Majority Vote*. Similarly each *ADV* is split so that the image is retained if incorrectly classified. Initially, for training the classifiers the full training set is used, and then the Walsh coefficient computation is reported for the split images.

Figs. 1-3 show classification error and Walsh decision probability as  $W_y$  is increased for  $d/c$ , and demonstrate the difference between clean and adversarial images (that is between *TR* and *ADVTR* and between *TE* and *ADVTE*).

Fig. 1a shows ensemble *TRcl1* and *DFTRcl2* average error versus order of Walsh coefficient for a twenty-one classifier ensemble. Figure 1b is similar to Fig. 1a, showing

error for *TRcl2* and *DFTRcl1*. Figs. 2a, 2b show the equivalent to Fig. 1 for Walsh decision probability. Note that for Fig. 1 the  $W_1$  *TR* error is 0 while *DFTR* error is 100 percent, since the data-set was split as explained above.

Figs. 3a, 3b show decision probability for *TE* versus *ADVTE* for all five *ADVs*. For *TEcl1* versus *ADVcl2* Figs. 2a, 3a show that Walsh probability is generally lower for *ADVcl2* with higher oscillations from odd to even coefficients. For *TEcl2* vs *ADVcl1* Figs. 2b, 3b show that Walsh probability is generally lower for *ADVcl1* and oscillations not as noticeable. Curves of *ADVs* in comparison with *TE* shown in Figs. 3a, 3b show similar trends to Figs. 2a, 2b indicating that transferability across classifiers trained on *ADVs* can be used to detect adversarial images.

From Figs. 3a, 3b there are various measures that could be used to potentially detect *ADVs*. For the set of experiments presented in this paper the second order coefficient  $W_2$  and the change from first to second order  $W_1/W_2$  is chosen for each dataset and each class. Fig. 4 shows *TR* and *TE* ensemble error using the full training/test set, demonstrating that the lowest test error occurs for  $W_1$  and  $W_2$ .

The difference between *TE* and *ADV* in Figs. 3a, 3b is an average, and in order to determine whether the difference can be used to detect *ADVs*, Fig. 5, shows a typical *TEACC/ADVREJ* curve as the  $W_1/W_2$  detection threshold is varied. A pattern is accepted if its probability is greater than probability threshold. The determination of the optimal threshold (0.125), which gives 87% for *TEcl1/DFcl2*, has not been investigated here. If *TR* was used to find the optimal value in this example, the threshold would be 0.15 giving *TEcl1/DFcl2* 85/92%. In practice, by using a validation set to find the optimal threshold, it should be possible to find a value between 87/87 and 85/92. By varying the threshold it would also be possible to alter the trade-off, for example from Fig. 5 *DFREJ* = 100% could potentially be achieved at *TEACC* = 80%.

Tables 2-5 show *TEACC* and *ADVREJ* for all problems considered from *CIFAR10* and *MNIST*. Numbers in the tables are italicised to indicate that  $W_2$  is chosen rather than  $W_1/W_2$ . No entry in the tables occurs when there are too few patterns that have been successfully attacked for a reliable estimate.

Table 2 shows the optimal *TEACC/ADVREJ* for all datasets in *CIFAR10* using *TEcl1/ADVcl2* and *TEcl2/ADVcl1*. Table 3 shows the values of *TEACC/ADVREJ* if the threshold is set by *DF* (for all datasets except *f/c*). From Table 3 it may be observed that the optimal thresholds for each *ADV* are similar, indicating that transferability of attack across classifiers is not strongly dependent on the particular attack. Table 4 shows the optimal values if *Majority Vote* is used for *TEcl1/ADVcl2*. In comparison with Table 2, the averages are much lower and there is much more variability among the different *ADVs*.

Table 5 shows the equivalent results for *MNIST* for *TEcl1/ADVcl2* and *TEcl2/ADVcl1*. However this is an easier data-set allowing perfect separation so that the optimal *TEACC/ADVREJ* for both class 1 and 2 may be obtained for all problems. The entries show the lower probability threshold and range over which both *TEACC* and *ADVREJ* are greater than 98 percent. It may be seen that the initial probability thresholds are very similar with high probability range (from 0.12 to 0.38

for *TEcl1/ADVcl2* and .15 to .52 for *TEcl2/ADVcl1*), indicating that it should be possible to locate the optimal *TEACC/ADVREJ*.

### 4.3 Discussion of Results

From Fig. 4 it may be seen that as the Walsh coefficient order is increased from  $W_{12} - W_{21}$  the generalisation becomes worse, so this is classic over-fitting as the decision boundary becomes more complex and *TR* can be learned perfectly. The best generalisation is found for  $W_1, W_2$  which is the reason why these were chosen for the experimental results shown in Tables 2 to 5. As may be seen in Fig. 4, the ensemble training error rate for  $W_{17} - W_{21}$  has dropped to zero, indicating a very complex boundary. However from Fig. 3 there is much better separation of the adversarial attacks at the higher order; so if higher order coefficients were chosen for the experiments, better separation on the adversarial attacks would be expected but at the cost of reduced *TE* classification accuracy. In Fig. 4, for  $W_{21}$  there is a loss of *TE* accuracy of approx. 6 percent compared with  $W_1$ . From the results in this section, it appears that the choice of Walsh coefficient order for optimal generalisation, may in general be different to that chosen for optimal adversarial robustness. The use of stronger *DNN* base classifiers should give even better results, but there would be a need to increase diversity for the ensemble to be effective. Understanding the trade-offs between accuracy, diversity and adversarial detection when using Walsh coefficients as an ensemble combining rule has not been considered in this paper.

Various approaches to rejecting adversarial examples can be found in the survey on rejection techniques in Zhang et al. [20]. A way to determine the optimal trade-off between accuracy and rejection could be to plot *security evaluation curves* (accuracy and rejection versus increase in attack perturbation) as proposed for the unified adversarial detection framework proposed in Crecchi et al. [21].

## 5 Conclusion

The main advantage of using Walsh approximation of an ensemble is that the complexity of the decision boundary can be controlled, and furthermore the output is a decision probability for a binary classification task. This is important for adversarial detection since, as explained in Section 3, one goal of adversarial perturbation applied to images is to push a pattern on the other side of a decision boundary, but not too far from the boundary, which could result in human-observable differences in the image. The approach in Guo et al. [41] relies on *prediction inconsistency* due to complicated decision boundaries to detect adversarial patterns; while similar to the approach proposed in this paper, only two *DNNs* with different architectures are used to determine prediction difference.

In practice most adversarial defences have been shown to fail assuming enough is known about defence details. Further work is required to determine how difficult it is to defeat a defence based on approximating an ensemble decision boundary using Walsh coefficients. It is not yet possible to describe such a defence as effective, since there has been no attempt to defeat it using an adaptive attack, that is one which is specifically designed to overcome the Walsh defence. A suggested way of overcoming

such a defence is to design a loss function based on all classifiers in the ensemble, as discussed in Tramèr et al. [6], for the ensemble defences [25] [26]. Even if an adaptive attack is successful, it is believed that using Walsh coefficient approximation will provide a tool that provides more insight into the training and transferability of *DNN* classifiers. A significant finding of this study is that transferability measured by Walsh approximation is very similar across different adversarial attacks. Also for two-class problems the two classes may show different transferability properties. Further investigation is needed to understand the relationship between transferability and correlation as measured by the Walsh approximation.

While the experiments here use images, the proposed approach of modelling two-class ensemble decision boundaries could in principle be applied to any application area. The analysis in this paper is restricted to two-class problems, but it may be easier to understand *DNNs* using two-class, before considering the more complex multi-class case. From a practical standpoint, it should be possible to scale the approach to multi-class using *Error-Correcting-Output-Codes (ECOC)* [26], which reduces multi-class problems to two class. Overall, further study is warranted into using Walsh coefficients for combining classifier decisions to model the ensemble decision boundary for adversarial robustness and for understanding *DNN* transferability and learning.

## References

- [1] Craighero F, Angaroni F, Stella F et al (2023) *Unity is strength: Improving the detection of adversarial examples with ensemble approaches*, Neurocomputing, Volume 554.
- [2] Han S, Lin C, Shen C et al (2023) *Interpreting Adversarial Examples in Deep Learning: A Review*, ACM Computing Surveys 55:14, Article 328, pp 1–38, <https://doi.org/10.1145/3594869>.
- [3] He K, Kim DD, Asghar MR (2023) *Adversarial Machine Learning for Network Intrusion Detection Systems: A Comprehensive Survey*, IEEE Communications Surveys & Tutorials 25:1, pp 538-566.
- [4] Nguyen K, Fernando T, Fookes C et al (2023) *Physical Adversarial Attacks for Surveillance: A Survey*, IEEE Transactions on Neural Networks and Learning Systems, doi: 10.1109/TNNLS.2023.3321432.
- [5] Ortiz-Jiménez G, Modas A, Moosavi-Dezfooli SM, Frossard P (2021) *Optimism in the Face of Adversity: Understanding and Improving Deep Learning through Adversarial Robustness*, Proceedings of the IEEE 109:5, pp 635-659.
- [6] Tramèr F, Carlini N, Brendel W, Madry A (2020) *On Adaptive Attacks to Adversarial Example Defenses*, Proceedings of NeurIPS, Vancouver, Canada, pp 1633-1645.
- [7] Wood D, Mu T, Webb AM et al (2023) *A unified theory of diversity in ensemble learning*. Journal of Machine Learning Research 24:359, pp 1-49.

- [8] Windeatt T (2006) *Accuracy/diversity and ensemble MLP classifier design*, IEEE Trans. Neural Netw., 17:5, pp 1194–1211.
- [9] He W, Wei J, Chen X et al (2017) *Adversarial example defense: Ensembles of weak defenses are not strong*, Proceedings of Workshop on Offensive Technologies.
- [10] Tou JT, Gonzales RC (1974) *Pattern Recognition Principles*, Addison-Wesley, pp 151-4.
- [11] Tikhonov AN, Arsenin VA (1977) *Solutions of Ill-posed Problems*, Winston & Sons, Washington, USA.
- [12] Hurst L, Miller DM, Muzio J (1985) *Spectral Techniques in Digital Logic*, Academic Press, NY, USA,.
- [13] Szegedy C, Zaremba W, Sutskever I, et al (2014) *Intriguing properties of neural networks*, arXiv:1312.6199v4.
- [14] Biggio B, Corona I, Maiorca D, et al (2017) *Evasion attacks against machine learning at test time*, Proceedings of ECMLPKDD, Lecture Notes in Computer Science 8190, Springer, Berlin.
- [15] Lin F (2022) *Learning in Neural Networks: Feedback-Network-Free Implementation and Biological Plausibility*, IEEE Trans. Neural Netw. Learn. Syst. 33:12, pp 7888–7898.
- [16] Goodfellow IJ, Shlens J, Szegedy C (2015) *Explaining and harnessing adversarial examples*, arXiv:1412.6572v3.
- [17] Shafahi A, Huang W, Studer C et al (2020) *Are adversarial examples inevitable?*, arXiv:1809.02104v3.
- [18] Schmidt L, Santurkar S, Tsipras D et al (2018) *Adversarially robust generalization requires more data*, Proceedings of NeurIPS.
- [19] Fawzi A, Moosavi-Dezfooli S, Frossard P (2016) *Robustness of classifiers: from adversarial to random noise*, Proceedings of NeurIPS.
- [20] Zhang X, Xie G, Li X et al (2023) *A Survey on Learning to Reject*, Proceedings of the IEEE 111:2.
- [21] Crecchi F, Melis M, Sotgiu A et al (2022) *FADER: Fast adversarial example rejection*, Neurocomputing 470, pp 257-268.
- [22] Zhang C, Benz P, Lin C et al (2022) *A Survey On Universal Adversarial Attack*, arXiv:2103.01498v2.

- [23] Ilyas A, Santurkar S, Tsipras D et al (2019) *Adversarial Examples are not Bugs, they are Features*, Proceedings of NeurIPS.
- [24] Pang T, Xu K, Du C et al (2019) *Improving adversarial robustness via promoting ensemble diversity*, Proceedings of ICML.
- [25] Sen S, Ravindran B, Raghunathan A (2020) *Ensembles of mixed precision deep networks for increased robustness against adversarial attacks*. arXiv:2004.10162v1.
- [26] Verma G, Swami A (2019) *Error correcting output codes improve probability estimation and adversarial robustness of deep neural networks*, Proceedings of NeurIPS.
- [27] Serban A, Poll E, Visser J (2020) *Adversarial Examples on Object Recognition: A Comprehensive Survey*, ACM Comp. Surveys 53:3, Art. No. 66, pp1-38.
- [28] Windeatt T, Zor C, Camgoz NC (2019) *Approximation of Ensemble Boundary Using Spectral Coefficients*, IEEE Trans. Neural Netw. Learn. Syst. 30:4, pp 1272-1277.
- [29] Tumer K, Ghosh J (1996) *Error correlation and error reduction in ensemble classifiers*, Connection Scienc 8:3, pp 385-404.
- [30] Windeatt T, Zor C (2011) *Minimising Added Classification Error Using Walsh Coefficients*, IEEE Trans. Neural Netw. 22:8, pp 1334-1339.
- [31] Windeatt T, Zor C (2013) *Ensemble pruning using spectral coefficients*, IEEE Trans. Neural Netw. Learn. Syst. 24:4, pp 673-678.
- [32] Nicolae M, Sinn M, Tran MN et al (2023) Adversarial Robustness Toolbox, arXiv:1807.01069v4 <https://adversarial-robustness-toolbox.readthedocs.io/en/latest/>.
- [33] Krizhevsky A, CIFAR-10 dataset (2023) [Online]. Available: <https://www.cs.toronto.edu/~kriz/cifar.html>.
- [34] Moosavi-Dezfooli S, Fawzi A, Frossard P et al (2016) *DeepFool: A Simple and Accurate Method to Fool Deep Neural Networks*, Proceedings of CVPR, pp 2574-2582.
- [35] Madry A, Makelov A, Schmidt L et al (2019) *Towards deep learning models resistant to adversarial attacks*, arXiv:1706.06083v4.
- [36] Moosavi-Dezfooli S, Fawzi A, Fawzi O et al (2017) *Universal adversarial perturbations*, Proceedings of CVPR, pp 1765-1773.



- [37] Kurakin A, Goodfellow I, Bengio S (2018) *Adversarial examples in the physical world*, Artificial Intelligence Safety and Security, Chapman and Hall/CRC.
- [38] Aldahdooh A, Hamidouche W, Fezza S et al (2022) *Adversarial example detection for DNN models: a review and experimental comparison*, Artificial Intelligence Review 55, pp 4403–4462.
- [39] Kwon H, Kim Y, Yoon H et al (2021) *Classification score approach for detecting adversarial example in deep neural network*, Multimedia Tools and Applications 80, pp 10339–10360.
- [40] LeCun Y, MNIST dataset (2023) [Online] Available: <http://yann.lecun.com/exdb/mnist/>.
- [41] Guo F, Zhao Q, Li X et al (2019) *Detecting adversarial examples via prediction difference for deep neural networks*, Information Sciences 501, pp 182-192.